New statistical methods enhance imaging of cameleon fluorescence resonance energy transfer in cultured zebrafish spinal neurons

Xiang Fan
Anirban Majumder
Sean S. Reagin
Erika L. Porter
The University of Georgia
Department of Cellular Biology
Athens, Georgia 30602

Andrew T. Sornborger
The University of Georgia
Department of Mathematics
and
Faculty of Engineering
Athens, Georgia 30602

Charles H. Keith*
The University of Georgia
Department of Cellular Biology
and
Faculty of Engineering
Athens, Georgia 30602

James D. Lauderdale*
The University of Georgia
Department of Cellular Biology
Athens, Georgia 30602

Abstract. Cameleons are genetically encoded fluorescence resonance energy transfer (FRET)–based Ca^{2+} indicators. Attempts to use cameleons to detect neural activity in vertebrate systems have been largely frustrated by the small FRET signal, in contradistinction to the higher signals seen in *Drosophila* and *Caenorhabditis elegans*. We have developed a statistical optimization method capable of detecting small ratiometric signals in noisy imaging data, called statistical optimization for the analysis of ratiometric signals. Using this method, we can detect and estimate anticorrelated ratiometric signals with subcellular resolution in cultured, dissociated zebrafish spinal neurons expressing cameleon or loaded with fluo-4 and fura-red. This method may make it possible to use yellow cameleons for measuring neural activity at high resolution in transgenic animals. [DOI: 10.1117/1.2745263]

Keywords: ratiometry; calcium; confocal microscopy; zebrafish.

Paper 06235SSR received Aug. 30, 2006; revised manuscript received Nov. 30, 2006; accepted for publication Dec. 1, 2006; published online May 31, 2007.

Introduction

A fundamental problem in neurobiology is to link behavior with neural activity. A full understanding of the neural mechanisms underlying behavior requires that we be able to monitor the activity of multiple neurons at a cellular level; however, this is difficult to accomplish using traditional electrophysiological methods. Alternate approaches use proxies for the electrical activity of cells. A particularly good example of such a proxy for the electrical activity of neurons is changes in intracellular calcium levels resulting from the influx of calcium through voltage-gated calcium channels.

The measurement of intracellular calcium levels in living cells can be accomplished through the use of synthetic calcium indicator dyes, such as fura-2 or fluo-4, which can be introduced into cells by bulk loading techniques such as ester loading or cell permeabilization, or by individual cell techniques, such as microinjection.[1] These dyes have proved extremely valuable in measuring changes in intracellular calcium in a wide variety of neuronal and nonneuronal cell types. However, most calcium indicators act as chelators and can affect the function of the cells of interest.[1] Furthermore, bulk loading techniques can damage cells and are difficult to restrict to particular types of cells in a tissue.

To circumvent these problems, genetically encoded calcium biosensors have been generated using variants of *Aequorea* green fluorescent protein (GFP).[2–6] Because genetically encoded biosensors can be selectively expressed, in principle, they should be able to dissect the activity of neural circuits in an intact animal more efficiently than synthetic calcium indicator dyes. Furthermore, when these dyes are expressed in an animal, animal viability and/or behavior offers an assay of whether they affect cell function.[7]

Cameleons are genetically encoded Ca^{2+} indicators (GECIs) based on fluorescent proteins and calmodulin (CaM).[8,9] They are chimeric proteins built of a short-wavelength variant of GFP (a fluorescence resonance energy transfer [FRET] donor), CaM, the CaM-binding peptide of myosin light-chain kinase (M13), and a long-wavelength variant of GFP (a FRET acceptor). Binding of Ca^{2+} to the CaM moiety initiates an intramolecular interaction between the CaM and M13 domains, causing the chimeric protein to shift from an extended conformation to a more compact one, thereby bringing the modified GFP domains close enough together to allow FRET

*Co-senior authors.
Address all correspondence to James D. Lauderdale, University of Georgia, Department of Cellular Biology, Athens, GA 30602; Tel: 706–542–3331; Fax: 706–542–4271; E-mail: jdlauder@cb.uga.edu

1083-3668/2007/12(3)/034017/7/$25.00 © 2007 SPIE

from the shorter-wavelength to the longer-wavelength variant of GFP.[10,11] This technique is useful for emission ratioing, which eliminates artifacts due to bleaching, variable illumination, and is more immune to movement or changes in focus than single-wavelength monitoring. Emission ratioing is an ideal readout for fast imaging by laser-scanning confocal microscopy.[3,7]

There are currently several different cameleons.[3,12,13] Yellow cameleons (YCs) have cyan and yellow fluorescent proteins (CFP and YFP) as the FRET donor and acceptor, respectively, and have been used to observe Ca^{2+} dynamics in the *Drosophila* neuromuscular junction,[14,15] mechanosensory neurons of *Caenorhabditis elegans*,[16] and sensory and spinal cord neurons in zebrafish.[7] YCs are classified into several groups based on the composition of their Ca^{2+} binding domains.[17] Of those that include the intact CaM, the YC2.1 version was used in zebrafish.[7]

Although cameleons were expected to be superior to synthetic dyes for investigating ensemble activity of neural circuitry in living animals, this expectation has been largely unmet in vertebrates. Even though YCs display robust Ca^{2+} responses *in vitro* and in transiently transfected cell samples, their dynamic range is significantly reduced in the nervous systems of transgenic vertebrates[3,4,13,18] and in primary neurons from vertebrates.[12] Most YCs, including YC2.1, exhibit at most a 120% change in the ratio of YFP/CFP upon Ca^{2+} binding in solution. However, this dynamic range appears to be attenuated in neuronal cell types that have a large amount of CaM and CaM-associated proteins, perhaps through interactions with the sensing domains of YCs.[19–21] Because of this problem, the successful use of YC in measuring stimulus-dependent responses in the Rohon-Beard neurons of transgenic zebrafish required extensive spatial averaging of fluorescence signals before ratiometric analysis.[7]

Because of the difficulties presented by cameleons, recent work in vertebrates has focused more on other GECIs, such as inverse pericam,[22] G-CaMP,[23] and Camgaroo-2,[24] which are single-wavelength indicators. Although these indicators have proved workable in vertebrate neurons[25] and nervous systems,[21,26] they forgo the benefits of ratiometric approaches. Additionally, this change, as well as the switch to improved cameleons,[12,13,19,20] leaves a large number of transgenic animals that are already expressing earlier versions of YCs unusable for functional imaging studies.

We recently developed an analytical technique that we called statistical optimization for the analysis of ratiometric signals (SOARS), which offers improved, user bias-independent detection of weak ratiometric signals at high resolution.[27] We have found that SOARS can reliably detect small changes in noisy imaging data in the ratio of YFP/CFP in cultured yellow cameleon-expressing zebrafish spinal neurons in response to high-potassium stimulation. This suggests that these techniques may enhance our ability to use YCs to detect stimulus-dependent activity in vertebrates.

Methods

Zebrafish Strains and Maintenance

Wild-type (WIK or TL) embryos were obtained from zebrafish (*Danio rerio*) lines maintained in the University of Georgia Zebrafish Facility following standard procedures.[28] WIK, and *Tuebingen long fin* (TL) were obtained from the Zebrafish International Resource Center (ZIRC). Zebrafish transgenic for the YC2.1 cameleon Ca^{2+} indicator[7] were originally obtained from Dr. Joe Fetcho (Cornell University, New York). Embryos were reared as previously described[28] and staged by hours post fertilization (hpf) at 28°C and by standard staging criteria.[29] Heterozygous *cameleon* embryos were generated by crosses between wild-type adults and adults heterozygous for *cameleon*.

Preparation of Dissociated Spinal Neuron Cultures

All experiments were performed in accordance with National Institutes of Health guidelines under protocols approved by the University of Georgia Animal Care and Use Committee. Dissociated zebrafish spinal neuron cultures were prepared from either wild-type embryos or embryos heterozygous for the *cameleon* transgene following established procedures.[30] Briefly, eggs collected from natural matings were bleached after collection and transferred to an embryo medium.[28] Embryos were allowed to develop to the 18-somite stage. *Cameleon* embryos were sorted by fluorescence using a stereomicroscope equipped for epifluorescence. Embryos were disinfected while still in their chorions with a 30-s rinse in a 70% ethanol solution, then transferred into Marc's modified Ringer's (MMR) medium.[30] The embryos were manually dechorionated, and the yolk sac and head were removed by mechanical dissection using sterilized forceps. The trunks from 10 to 14 embryos were transferred to 15-ml conical centrifuge tubes containing 5 ml of custom ATV solution (Irvine Scientific, Irvine, California)[30] and incubated at room temperature for 9 min. The cells were collected by low-speed centrifugation
(3 min at 720 rpm) in a clinical centrifuge. The supernatant was carefully removed, and the cell pellet resuspended in 0.5 ml-culture medium.[30] The cells were plated on either acid-washed or laminin-coated 25-mm round coverslips and cultured at room temperature in the dark. The neurons in these cultures remained viable for up to 7 days. We typically imaged neurons cultured for 3 days.

For calcium measurements in wild-type neurons, the cultured neurons were bulk loaded immediately before imaging with 1-μM fluo-4 (Invitrogen/Molecular Probes, Eugene, Oregon F14217) and 10-μM fura-red (Invitrogen/Molecular Probes, F3021) acetoxymethyl (AM) ester fluorescent indicator dyes in a 60% dilution of Hanks' balanced salt solution (HBSS),[31] 0.04% pluronic F-127 (Invitrogen/Molecular Probes, P6867) for 20 min at room temperature. After loading, the cells were rinsed with 60% HBSS and mounted in a Dvorak-Stottler chamber (Lucas-Highland, Chantilly, Virginia). For calcium measurements in cameleon-expressing neurons, coverslips were rinsed in 60% HBSS and mounted in a Dvorak-Stottler chamber.

Confocal Microscopy

Confocal microscopy was performed on a Leica SP2 confocal microscope on a Leica DM RXE upright microscope (Leica Microsystems, Bannerbrook, Illinois). Excitation of cameleon-expressing cells was with the 458-nm line of a 50-mW argon laser, with emission bands of 40 and 30 nm, centered around 485 (cyan) and 535 (yellow) nm, respec-

tively. Cells were maintained in a Dvorak-Stottler chamber and perfused at a rate of 8.3 μl/s with 60% HBSS, alternating with a 60% dilution of a modified HBSS, with 30-mM KCl substituting for 30 mM of the normal NaCl (high-K^+ HBSS). Images were taken with the acoustic optical beamsplitter set to deliver 5 to 7% of the laser intensity. This excitation level was generally sufficient to excite approximately 10% of the pixels in the cyan image, and a few pixels in the yellow image, to saturation (gray level 255 in an 8-bit image). The photomultiplier gain in each channel was then adjusted downward to eliminate saturated pixels. Images for ratiometric analyses were collected at a rate of 1/s, at a scale of 256 $\times$ 256 pixels. Cells were perfused alternately with HBSS and high-K^+ HBSS, switching at 2-min intervals, for a total of 10 cycles. Subsequently, they were perfused for 5 min with HBSS containing 10-μM ionomycin (Invitrogen/Molecular Probes) and 10-mM ethylene glycol tetraacetic acid (EGTA) (low calcium clamp), and then for 5 min with HBSS containing 10-μM ionomycin and saturated Ca^{2+}. In some cases, a separate data series was taken in which cells were perfused with 2-min pulses of HBSS alternating with HBSS +0.0005% fluorescein, so that the perfusion profile of the chamber could be established.

Wild-type neurons loaded with fluo-4 and fura-red were imaged in the same fashion as cameleon-expressing neurons, except that the excitation was at 488 nm, and emission was at 516 and 655 nm from fluo-4 and fura-red, respectively.

Before each series of wild-type neurons loaded with fluo-4 and fura-red, high-resolution images were collected in HBSS (nonstimulated) and High-K HBSS (stimulated) conditions (Fig. 2). These images were taken at a scale of 1024 $\times$ 1024 pixels, at a 10% laser intensity, with 8-fold image averaging. With cameleon-expressing neurons, only a single high-resolution image was taken because of concerns that we might engender rapid bleaching of the YC.[7]

Data Analysis

Due to the low signal-to-noise ratio (SNR) of approximately 1/10, ratiometric imaging data was analyzed with the multivariate SOARS method that we have developed. Although the technical details of SOARS will be published elsewhere,[27] MATLAB code is available upon request. Here we provide a description of SOARS.

To describe SOARS, we begin by noting that both fluorescence data sets are taken of exactly the same spatial region. By standardizing the two data sets, one now has two data sets in which, if there is a signal, pixel time courses in one data set will trend upward when pixels in the other data set trend downward (i.e., the signal is anticorrelated). By subtracting the two data sets, pixel by pixel, one forms a single data set in which any consistent trend away from zero indicates anticorrelation in the data. Performing a singular value decomposition (SVD) on the standardized, subtracted data set results in a set of eigenimages that are ordered by the amount of spatial covariance in the data. The time courses of the eigenimages in the standardized, subtracted data set will be normally distributed under the null hypothesis (i.e., if no anticorrelation exists, and it is not normally distributed otherwise). The time courses of the eigenimages in the original data sets after standardization will be anticorrelated if there is a signal. That is, the nonnormal eigenimages represent weighted masks showing the spatial distribution of anticorrelation in the data set. It should be noted that the SVD eigenimages form a complete basis for the standardized, subtracted data set. Therefore, in principle, one can completely reconstruct that data set via a combination of all of the eigenimages. SOARS is a filtering method because it throws away any eigenimages that do not correspond to anticorrelated information. Therefore, it filters the data set in a subspace that contains only anticorrelated information. Because SOARS provides a *set* of masks, one is able to visualize spatiotemporal dynamics in the imaging data. SOARS thereby avoids the loss of spatial information that comes with averaging over regions of interest (ROIs). By projecting the eigenimages into the original data sets after standardization, one effectively denoises the data in both channels. Multiplying by the standard deviation and adding the mean back into the data sets, one now has data sets at two wavelengths that have been restricted to contain only anticorrelated information from which ratios may be taken. The reconstruction of the ratio is, at this point, denoised to the extent possible given the statistical model and the statistical optimization framework within which SOARS is working.

Given the above discussion, a SOARS analysis consists of four main steps: (1) Standardization and subtraction of the fluorescence signals from two wavelengths. (2) Performance of a SVD on the standardized, subtracted data. (3) Statistical selection of eigenimages. (4) Reconstruction of the ratio using only statistically significant eigenimages (a denoised, or optimally filtered, ratio).

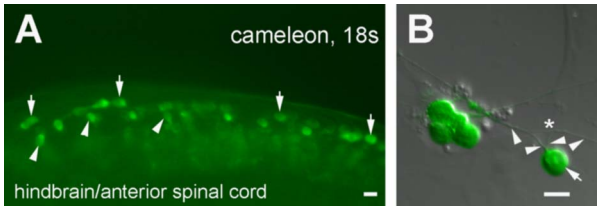

Fig. 1 Dissociated spinal neurons express cameleon in culture. (a) Side view of the posterior hindbrain and anterior spinal cord of a heterozygous *cameleon* embryo at 18 somites (18s). Anterior is to the left and dorsal is up. Arrows denote putative RB sensory neurons and arrowheads denote commissural neurons. (b) Dissociated spinal neurons express *cameleon* after 3 days in culture. The neuron denoted with an arrow has a large soma and has extended two thin axons from one side of the cell body (arrowheads); one of these axons has formed a sidebranch (asterisk). This morphology is characteristic of RB neurons (Ref. 34). Scale bars: 10 μm.

Results

Dissociated Spinal Neurons Express Cameleon in Culture

In the line of transgenic fish used for these experiments, cameleon is expressed under the control of the HuC promoter and is therefore expressed in all neurons.[7,32] The neuronal specificity of cameleon expression is apparent in Fig. 1(a), in which only approximately 16 cells in the cross section of expressed cameleon, and many of these cells have obvious neuritic processes. The neuronal specificity of cameleon was also verified by double-labeling cameleon-expressing cells using an antibody for acetylated tubulin,[33] which labels most, if

not all, neurons and their axons in zebrafish.[34–36] This antibody immunolabeled all cameleon-expressing cells (data not shown). At the time that the dissections are performed [18 to 20 hours post-fertilization (hpf)], the spinal cord contains at least five classes of neurons, including the Rohon-Beard (RB) mechanosensory neurons, commissural primary ascending (CoPA) neurons, ventral longitudinal descending, dorsal longitudinal ascending, and primary motor neurons.[34] RB neurons and commissural neurons are both clearly visible in the embryo at this stage [Fig. 1(a)]. RB neurons have large somata (~9 μm in diameter; ~64 μm^2), which are located in the dorsal-most neural tube and extend two thin axons from the ventral side of the cell body; one of these axons forms a sidebranch, which is usually located near the soma.[34] There are several types of commissural neurons, all of which project axons to the ventral midline of the neural tube. Of these, the commissural primary ascending (CoPA) neurons have a distinctive morphology, which aids in the identification of these neurons. CoPA commissural neurons tend to have spherical soma of ~89 μm^2 with three unbranched processes, giving the neuron a characteristic T shape.[34]

We tested if dissociated spinal neurons continued to express *cameleon* in culture. Dissociated zebrafish spinal neuron cultures[30] were prepared from embryos heterozygous for the *cameleon* transgene. This procedure produces a heterogeneous population of cells, which includes epithelial or fibroblast cells, myocytes, and neurons (data not shown, see also Ref. 30). Because of the way the dissection was performed, the culture likely also contained trunk neural crest cells, which are migrating from the dorsal neural tube at this time.[37] Of these only neurons expressed cameleon [Fig. 1(b)]. We observed cameleon-expressing neurons with different morphologies, including unipolar and bipolar neurons and putative RBs [Fig. 1(b) and data not shown].

Imaging Dissociated Zebrafish Spinal Neurons Loaded with Fluo-4 and fura-red

Our objective was to test if SOARS[27] could be used to reliably detect a FRET signal at high resolution in cameleon-expressing spinal neurons in response to stimulation. As a first step, we tested the response of dissociated wild-type zebrafish spinal neurons in culture to depolarizing conditions (Fig. 2). These cells were bulk loaded with fluo-4 and fura-red (Fig. 2). Fluo-4 and fura-red are calcium indicators that make a ratiometric pair. Whereas fluo-4 fluorescence increases with increasing $[Ca^{2+}]$, fura-red's fluorescence decreases.[38–40] Exposure of neurons to K^+-containing solutions causes depolarization of the cells and a rise in the free intracellular Ca^{2+} concentration ($[Ca^{2+}]_i$) through the action of voltage-gated channels in the plasma membrane.[41–43] As expected, neurons exposed to a 30-mM KCl solution exhibited an increase in fluo-4 fluorescence and a concomitant decrease in fura-red fluorescence (Fig. 2). Consistent with published reports in other types of neurons, these experiments indicated that exposure of cultured zebrafish spinal neurons to these depolarizing conditions resulted in a measurable increase in $[Ca^{2+}]_i$.

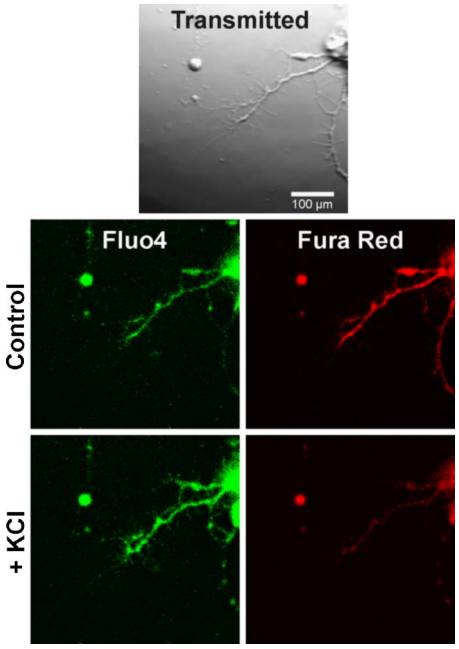

Fig. 2 Fluorescence images of dye-loaded zebrafish neurons and neurites in culture. The AM esters of fluo-4 and fura-red were used to bulk load dissociated spinal neurons. Fluo-4 fluorescence increased and fura-red fluorescence decreased in response to exposure to KCl, which causes depolarization of the neurons and an increase in $[Ca^{2+}]_i$. Scale bar in transmitted light image applies to all panels.

Imaging Dissociated Cameleon-Expressing Neurons in Culture

We next measured the response of cameleon-expressing neurons to stimulation (Fig. 3). In these experiments, the cultured neurons were periodically stimulated with a 60% dilution of HBSS containing 30-mM KCl (2 min off/2 min on) for 10 periods (40 min total). At the end of each experiment, response to Ca^{2+} was calibrated by exposure to an ionomycin solution containing EGTA followed by ionomycin plus saturating Ca^{2+} [Fig. 3(d)]. Transmitted light was measured in a transmission photo multiplier tube and used to detect any motion in the cells (data not shown).

The FRET fluorescence data was analyzed using the SOARS method.[27] This is a statistical optimization method for denoising ratiometric data by detecting spatially correlated, temporally anticorrelated information in the two channels being imaged. The method results in a set of statistically significant eigenimages whose projection in the data is maximally anticorrelated. Typically, the first few eigenimages capture the response to stimulation. We show one such eigenimage [Fig. 3(b)] along with the anticorrelated time courses of the CFP and YFP channels [Fig. 3(c)]. The eigenimage in Fig. 3(b) shows that, even though the mean fluorescence is largest in the cell bodies, the part of the FRET response captured in this eigenimage is fairly even throughout the cell, although some subcellular structure (lighter and darker regions) is visible. The neurites that are readily visible in the eigenimage are only 3 to 4 pixels in width.

Our experimental paradigm makes it particularly simple to identify the response to stimulus [Fig. 3(c)] because it results in a characteristic periodic epoch, followed by large changes

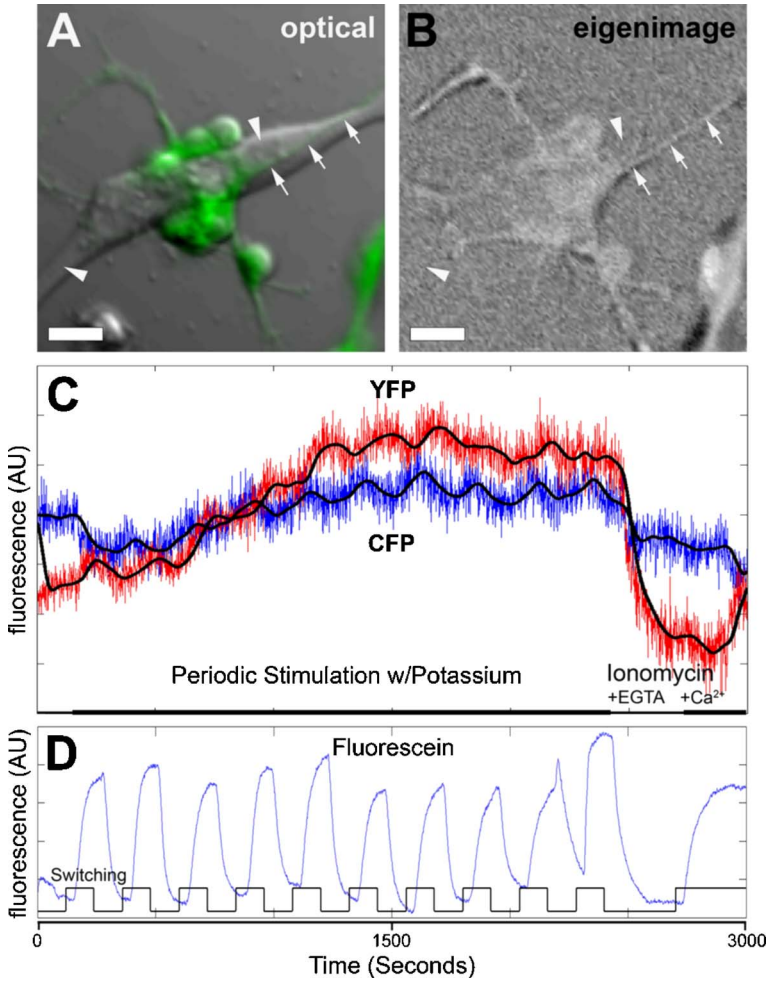

Fig. 3 SOARS analysis of the FRET response of cameleon-expressing neurons to stimulation. (a) Optical (transmitted light) image overlaid with fluorescence image of zebrafish neurons and a fibroblast in culture. Note that only neurons express cameleon. Mean YFP fluorescence is shown in green. An axon extending along the fibroblast is denoted with arrows and the fibroblast is denoted with arrowheads. (b) and (c) Results of a SOARS analysis on FRET imaging data of the response of cameleon-expressing neurons to our stimulation paradigm [see panel (d)]. (b) Weighted mask (eigenimage) resulting from SOARS analysis of the FRET data. This eigenimage represents spatially correlated, temporally anticorrelated information in the data set. No morphological information was used to generate this image (see Ref. 27). (c) The projections (time courses) of the weighted mask in the CFP and YFP data sets. The anticorrelated emission fluorescence of CFP and YFP is evident. (d) Stimulation paradigm: solutions were changed every two minutes for 10 periods, followed by 5-min exposure to ionomycin plus EGTA, followed by exposure to ionomycin plus Ca^{2+} (switching, black trace). Stimulus concentration time course was visualized by flowing fluorescein through the Dvorak-Stottler chamber (blue trace). Note the time lag between on and off switches and the corresponding change in fluorescein concentration. Scale bar: 40 μm.

due to the ionomycin plus EGTA "low calcium clamp." As well as these obvious features, there is an apparent slow increase in Ca^{2+} over time. No FRET response is seen in a negative control (alternate exposure to nonpotassium containing solutions, data not shown).

Reconstruction of a Denoised Ratio with SOARS

Ratiometric signals may be used to obtain quantitative information on Ca^{2+} concentrations. Ratioing also eliminates fluorescence excitation fluctuations due to the illumination source, eliminates the effects of bleaching, and ameliorates motion artifacts. However, quantitative information can be wildly inaccurate in noisy data, particularly due to noise in the denominator of the ratio: Noise fluctuations can give spurious low values in the denominator and consequent spikes in the ratio. SOARS is an effective method for denoising the data, which leads to a more accurate estimate of the ratio.

Only one of the statistically significant eigenimages was presented in Fig. 3. In Fig. 4, we show a complete reconstruction of the ratio using *all* of the statistically significant eigenimages from the SOARS analysis. Without experience, eigenimages can be difficult to interpret because they are a transformed representation of the data. Therefore, Fig. 4 depicts the reconstructed ratio in space from stimulus onset to peak response. To make the reconstruction, the first five eigenimages from the SOARS analysis and their time courses were used. The movie is dominated by the first eigenimage [see Fig. 3(b)], but small dynamical changes due to the other statistically significant eigenimages are also included in the reconstruction. Whereas one eigenimage [e.g., Fig. 3(b)] often captures the dominant response, subtle statistically significant

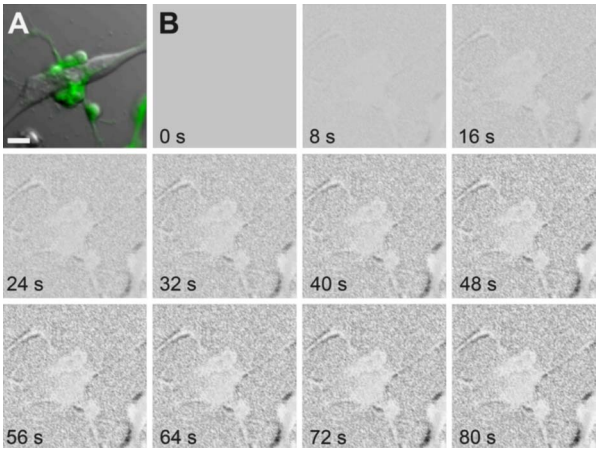

Fig. 4 A SOARS estimate of the dynamics of the Ca^{2+} response in zebrafish neurons. (a) Optical (transmitted light) image overlaid with fluorescence image of zebrafish neurons and a fibroblast in culture. (b) The SOARS denoised, spatiotemporal reconstruction of the ratio shown over slightly less than one stimulus interval (approximately from baseline to maximal response). Depicted is the deviation of the ratio from the baseline ratio (i.e., the initial frame is subtracted from subsequent frames). Plotting this differential response as a function of time allows us to better see the dynamics of the ratio as the neurons respond to a depolarizing solution. Whereas the intensity of the cameleon fluorescence is higher in the soma relative to the neurites (a), the ratiometric FRET response to calcium is more uniform throughout the neuron, indicating a uniform Ca^{2+} increase throughout the cell. Scale bar: 40 μm; applies to all panels.

quantitative information concerning the FRET response is captured by a few other eigenimages. The dominance of the first eigenimage here is most likely due to the fact that the K^+ stimulus is spatially uniform in this experiment. If local dynamical events, such as calcium waves, had been evoked, then higher order eigenimages would have contributed more to the reconstruction. This additional information can provide insight into physiological changes in the preparation that might well go unseen in the absence of a SOARS analysis.

Discussion

SOARS is a method that we have developed to detect and estimate weak signals in ratiometric imaging data. It is based on a statistical optimization procedure that identifies maximally spatially correlated and temporally anticorrelated information in two-channel ratiometric imaging data. Standard methods rely on user-defined data masks (ROIs) to reduce the SNR by averaging over pixels. Although ROI methods are easy to use, there can be significant disadvantages to using this approach (see Ref. 27). A major advantage of using SOARS is that user-defined masks (ROIs), which are determined subjectively by the analyst, are replaced by eigenimages (weighted masks) that are objectively calculated using optimization methods from the data. SOARS results in a set of eigenimages along with their time courses that may be used to reconstruct (then ratio) two denoised data sets. Because multiple eigenimages are used in the reconstruction, high-resolution spatial and temporal information is retained in the estimated ratio.

The ability to use genetically encoded indicators of neural activity at cellular and subcellular scales is necessary for the analysis of the activity of entire neuronal circuits and provides both more local and global information in comparison to standard electrophysiological measurements of neuronal activity. A useful model for imaging a complete vertebrate neural system is the YC2.1 transgenic zebrafish. However, it is known that the cameleon signal in zebrafish is weak. We have applied SOARS to the analysis of cameleon FRET data to highlight the method's usefulness for detecting weak ratiometric signals and to help rescue zebrafish and other vertebrate models for neural studies. As a first step, in this *in vitro* study, we corroborate the *in vivo* results of Higashijima and colleagues[7] that indicate that panneurally expressed YC2.1 can be used to indicate neural activity in zebrafish neurons. In our ratio reconstruction, neurites with a spatial width of 3 to 4 pixels ($\leq$1 μm) are readily visible. In Higashijima et al.,[7] the ratio estimate analysis was performed by averaging over a ROI of approximately 2000 pixels (a cell body of approximately 9 μm in diameter). Such averaging destroys information on smaller scales, whereas SOARS retains fine resolution in the ratio estimate. Because of our analytical techniques and experimental design, we are able to extend the spatiotemporal characterization of the cameleon response to the subcellular scale of resolution ($\leq$1 μm in Fig. 3). Although this study was performed using dissociated zebrafish spinal neurons in culture, we have applied the SOARS method to detect neural activation in intact zebrafish with similar results.[44]

Despite their low SNR in transgenic vertebrates, yellow cameleons are valuable tools for measuring neural activity:

- Cameleons are inherently ratiometric and thus give measurements that are relatively insensitive to variations in tissue thickness and focus.[3]
- Cameleons (and other GECIs) are built around calmodulin, or other calcium-binding proteins, rather than 1,2-bis(*o*-aminophenoxy) ethane-N,N,N',N'-tetraacetic acid or BAPTA. They therefore have K_d's for the binding of calcium in the 0.1-1-μM to range, and buffer intracellular calcium less than many synthetic calcium indicators.[1] In one experiment, fura-red loading into cameleon-expressing neurons completely damped the periodic Ca^{2+} response, but left the EGTA low calcium clamp intact (data not shown), suggesting that fura-red was buffering calcium in the cell.
- GECIs can be introduced into cells or organisms in ways that do not injure the neurons of interest. Any deleterious effects they may have on cellular or organismal function can be readily assessed.[7] Furthermore, by using tissue-specific promoters, GECIs can be selectively expressed in tissues or cell types of interest.
- Existing organisms transgenic for *cameleons* are currently available,[7,14,16] and can be used without investing the time to generate new transgenic lines.

Our results demonstrate the ability of SOARS to detect weak ratiometric signals in YC2.1 imaging data. This method is equally applicable to any ratiometric imaging data, including those obtained with the synthetic ratiometric dyes di-4,8-Anepps, indo-1,5F and fura-2,3,4F, as well as intrinsic ratiometric signals such as reduced nicotinamide adenine dinucleotide (NADH)/flavoprotein fluorescence and other genetically encoded ratiometric indicators. The newer genera-

tion of GECIs[3,20,21,26,45] should prove to be particularly powerful for imaging neural activity due to the improved quantum yields of the indicators. In combination with SOARS, these indicators may become even more useful for detecting the subtleties of neural activity in noisy measurements.

Efforts to generate mice transgenic for cameleons have, to our knowledge, been unsuccessful to date, and in cases where mosaic expression of YCs is seen, existing analytical techniques have yielded only small functional signals.[21,46] Our experience in other systems[27] suggests that SOARS, particularly when used in a repetitive-stimulus paradigm, may allow us to use YC, even in these challenging systems.

Acknowledgments

This work was supported by faculty research grants (ATS, JDL), a University of Georgia engineering grant (ATS, CHK, JDL) from the University of Georgia Research Foundation, and a National Institutes of Health grant EB005432 (ATS, CHK, JDL). The authors wish to thank J. R. Fetcho (Cornell University) for the gift of zebrafish expressing YC2.1.

References

1. A. Takahashi et al., "Measurement of intracellular calcium," *Physiol. Rev.* **79**(4), 1089–1125 (1999).
2. J. Zhang et al., "Creating new fluorescent probes for cell biology," *Nat. Rev. Mol. Cell Biol.* **3**(12), 906–918 (2002).
3. A. Miyawaki, "Innovations in the imaging of brain functions using fluorescent proteins," *Neuron* **48**(2), 189–199 (2005).
4. A. Miyawaki et al., "Development of genetically encoded fluorescent indicators for calcium," *Methods Enzymol.* **360**, 202–225 (2003).
5. G. Miesenböck, "Genetic methods for illuminating the function of neural circuits," *Curr. Opin. Neurobiol.* **14**(3), 395–402 (2004).
6. G. Miesenböck and I. G. Kevrekidis, "Optical imaging and control of genetically designated neurons in functioning circuits," *Annu. Rev. Neurosci.* **28**, 533–563 (2005).
7. S. Higashijima et al., "Imaging neuronal activity during zebrafish behavior with a genetically encoded calcium indicator," *J. Neurophysiol.* **90**(6), 3986–3997 (2003).
8. A. Miyawaki et al., "Fluorescent indicators for Ca2+ based on green fluorescent proteins and calmodulin," *Nature (London)* **388**(6645), 882–887 (1997).
9. R. Y. Tsien, "The green fluorescent protein," *Annu. Rev. Biochem.* **67**, 509–544 (1998).
10. G. H. Patterson, D. W. Piston, and B. G. Barisas, "Forster distances between green fluorescent protein pairs," *Anal. Biochem.* **284**(2), 438–440 (2000).
11. S. Habuchi et al., "Resonance energy transfer in a calcium concentration-dependent cameleon protein," *Biophys. J.* **83**(6), 3499–3506 (2002).
12. K. Truong et al., "FRET-based in vivo Ca2+ imaging by a new calmodulin-GFP fusion molecule," *Nat. Struct. Biol.* **8**(12), 1069–1073 (2001).
13. T. Nagai et al., "Expanded dynamic range of fluorescent indicators for Ca(2+) by circularly permuted yellow fluorescent proteins," *Proc. Natl. Acad. Sci. U.S.A.* **101**(29), 10554–10559 (2004).
14. D. F. Reiff et al., "In vivo performance of genetically encoded indicators of neural activity in flies," *J. Neurosci.* **25**(19), 4766–4778 (2005).
15. G. Guerrero et al., "Heterogeneity in synaptic transmission along a Drosophila larval motor axon," *Nat. Neurosci.* **8**(9), 1188–1196 (2005).
16. H. Suzuki et al., "In vivo imaging of C. elegans mechanosensory neurons demonstrates a specific role for the MEC-4 channel in the process of gentle touch sensation," *Neuron* **39**(6), 1005–1017 (2003).
17. A. Miyawaki, "Visualization of the spatial and temporal dynamics of intracellular signaling," *Dev. Cell* **4**(3), 295–305 (2003).
18. A. Miyawaki et al., "Dynamic and quantitative Ca2+ measurements using improved cameleons," *Proc. Natl. Acad. Sci. U.S.A.* **96**(5), 2135–2140 (1999).
19. A. E. Palmer et al., "Bcl-2-mediated alterations in endoplasmic reticulum Ca2+ analyzed with an improved genetically encoded fluorescent sensor," *Proc. Natl. Acad. Sci. U.S.A.* **101**(50), 17404–17409 (2004).
20. N. Heim and O. Griesbeck, "Genetically encoded indicators of cellular calcium dynamics based on troponin C and green fluorescent protein," *J. Biol. Chem.* **279**(14), 14280–14286 (2004).
21. M. T. Hasan et al., "Functional fluorescent Ca2+ indicator proteins in transgenic mice under TET control," *PLoS Biol.* **2**(6), 763–775 (2004).
22. T. Nagai et al., "Circularly permuted green fluorescent proteins engineered to sense Ca2+," *Proc. Natl. Acad. Sci. U.S.A.* **98**(6), 3197–3202 (2001).
23. J. Nakai, M. Ohkura, and K. Imoto, "A high signal-to-noise Ca(2+) probe composed of a single green fluorescent protein," *Nat. Biotechnol.* **19**(2), 137–141 (2001).
24. O. Griesbeck et al., "Reducing the environmental sensitivity of yellow fluorescent protein. Mechanism and applications," *J. Biol. Chem.* **276**(31), 29188–29194 (2001).
25. T. A. Pologruto, R. Yasuda, and K. Svoboda, "Monitoring neural activity and [Ca2+] with genetically encoded Ca2+ indicators," *J. Neurosci.* **24**(43), 9572–9579 (2004).
26. J. Li et al., "Early development of functional spatial maps in the zebrafish olfactory bulb," *J. Neurosci.* **25**(24), 5784–5795 (2005).
27. J. Broder et al., "Estimating weak ratiometric signals in imaging data I: Dual-channel data," *J. Opt. Soc. Am. A* (in press).
28. M. Westerfield, Ed., *The Zebrafish Book: A Guide for the Laboratory Use of Zebrafish (Danio rerio)*, 4 ed., University of Oregon Press, Eugene (2000).
29. C. B. Kimmel et al., "Stages of embryonic development of the zebrafish," *Dev. Dyn.* **203**(3), 253–310 (1995).
30. S. S. Andersen, "Preparation of dissociated zebrafish spinal neuron cultures," *Methods Cell. Sci.* **23**(4), 205–209 (2001).
31. J. Hanks, "Hanks' balanced salt solution and pH control," *Tissue Culture Association Manual*, Vol. 3, pp. 3–15 (1976).
32. H. C. Park et al., "Analysis of upstream elements in the HuC promoter leads to the establishment of transgenic zebrafish with fluorescent neurons," *Dev. Biol.* **227**(2), 279–293 (2000).
33. G. Piperno and M. T. Fuller, "Monoclonal antibodies specific for an acetylated form of alpha-tubulin recognize the antigen in cilia and flagella from a variety of organisms," *J. Cell Biol.* **101**, 2085–2094 (1985).
34. R. R. Bernhardt et al., "Identification of spinal neurons in the embryonic and larval zebrafish," *J. Comp. Neurol.* **302**(3), 603–616 (1990).
35. A. B. Chitnis and J. Y. Kuwada, "Axonogenesis in the brain of zebrafish embryos," *J. Neurosci.* **10**(6), 1892–1905 (1990).
36. J. D. Lauderdale, N. M. Davis, and J. Y. Kuwada, "Axon tracts correlate with netrin-1a expression in the zebrafish embryo," *Mol. Cell. Neurosci.* **9**(4), 293–313 (1997).
37. D. W. Raible et al., "Segregation and early dispersal of neural crest cells in the embryonic zebrafish," *Dev. Dyn.* **195**(1), 29–42 (1992).
38. P. Lipp and E. Niggli, "Ratiometric confocal Ca(2+)-measurements with visible wavelength indicators in isolated cardiac myocytes," *Cell Calcium* **14**(5), 359–372 (1993).
39. J. Bischofberger and D. Schild, "Different spatial patterns of [Ca2+] increase caused by N- and L-type Ca2+ channel activation in frog olfactory bulb neurones," *J. Physiol. (London)* **487**(2), 305–317 (1995).
40. T. M. Gomez et al., "Filopodial calcium transients promote substrate-dependent growth cone turning," *Science* **291**(5510), 1983–1987 (2001).
41. R. J. Miller, "Multiple calcium channels and neuronal function," *Science* **235**(4784), 46–52 (1987).
42. R. W. Tsien et al., "Multiple types of neuronal calcium channels and their selective modulation," *Trends Neurosci.* **11**(10), 431–438 (1988).
43. R. J. Miller, "Calcium signalling in neurons," *Trends Neurosci.* **11**(10), 415–419 (1988).
44. A. Majumder, C. H. Keith, A. T. Sornborger, and J. D. Lauderdale, unpublished.
45. A. Miyawaki, T. Nagai, and H. Mizuno, "Engineering fluorescent proteins," *Adv. Biochem. Eng./Biotechnol.* **95**, 1–15 (2005).
46. P. S. Tsai et al., "All-optical histology using ultrashort laser pulses," *Neuron* **39**(1), 27–41 (2003).